Elsevier required licence: © <2021>. This manuscript version is made available under the CC-BY-NC-ND 4.0 license http://creativecommons.org/licenses/by-nc-nd/4.0/
The definitive publisher version is available online at https://doi.org/10.1016/j.memsci.2021.119567

# Control of the antagonistic effects of heat-assisted chlorine oxidative degradation on pressure retarded osmosis thin film composite membrane surface

*Ralph Rolly Gonzales*[a,b], *Ahmed Abdel-Wahab*[c], *Dong Suk Han*[d], *Hideto Matsuyama*[b], *Sherub Phuntsho*[a], *Ho Kyong Shon*[a*]

[a]Centre for Technology in Water and Wastewater, University of Technology Sydney, New South Wales, Australia

[b]Research Center for Membrane and Film Technology, Kobe University, Kobe, Hyogo, Japan

[c]Chemical Engineering Program, Texas A & M University at Qatar, Education City, Doha, Qatar

[d]Center for Advanced Materials, Qatar University, Doha, Qatar

*Corresponding author: Ho Kyong Shon; Email: hokyong.shon-1@uts.edu.au

## Abstract

During pressure retarded osmosis (PRO) operation, thin film composite (TFC) membranes are continuously exposed to chemicals present in the stream that can deteriorate the membrane's selective layer with exposure time. Following this observation, TFC membranes are placed in controlled oxidative degradation conditions using aqueous NaOCl solutions. Active chlorine, along with heat, can thin out the dense layer and, when controlled and optimized, can tune the membrane surface properties and separation efficiency as desirable for specific applications. The chlorine oxidative degradation is optimized in terms of chlorine exposure (a factor of both exposure time and chemical dosage), solution pH, and the subsequent heating time. After the chemical modification process, the membrane surface properties were characterized and the PRO performance as well as the osmotic energy harvesting capability were determined. The modified membranes exhibited different levels of polyamide degradation and increase in water permeability, which came along with decrease in selectivity. Optimization of the chlorine oxidative degradation using response surface methodology was performed to maximize the water permeability and extractable osmotic power while keeping salt rejection satisfactory. After performing chlorine oxidation at the following optimized conditions: 3025 ppm $Cl_2 \cdot h$, pH 10.72, and 3 min heating time, initial non-pressure retarded water flux of 73.2 L $m^{-2}$ $h^{-1}$, specific reverse solute flux of 1.17 g $L^{-1}$, and power density of 18.71 W $m^{-2}$ (corresponding to water flux of 56.1 L $m^{-2}$ $h^{-1}$) at 12 bar were obtained using 0.6 M NaCl as draw and deionized water as feed.



## Keywords

pressure retarded osmosis; thin film composite membrane; chlorine; oxidative degradation; response surface methodology

## Graphical abstract

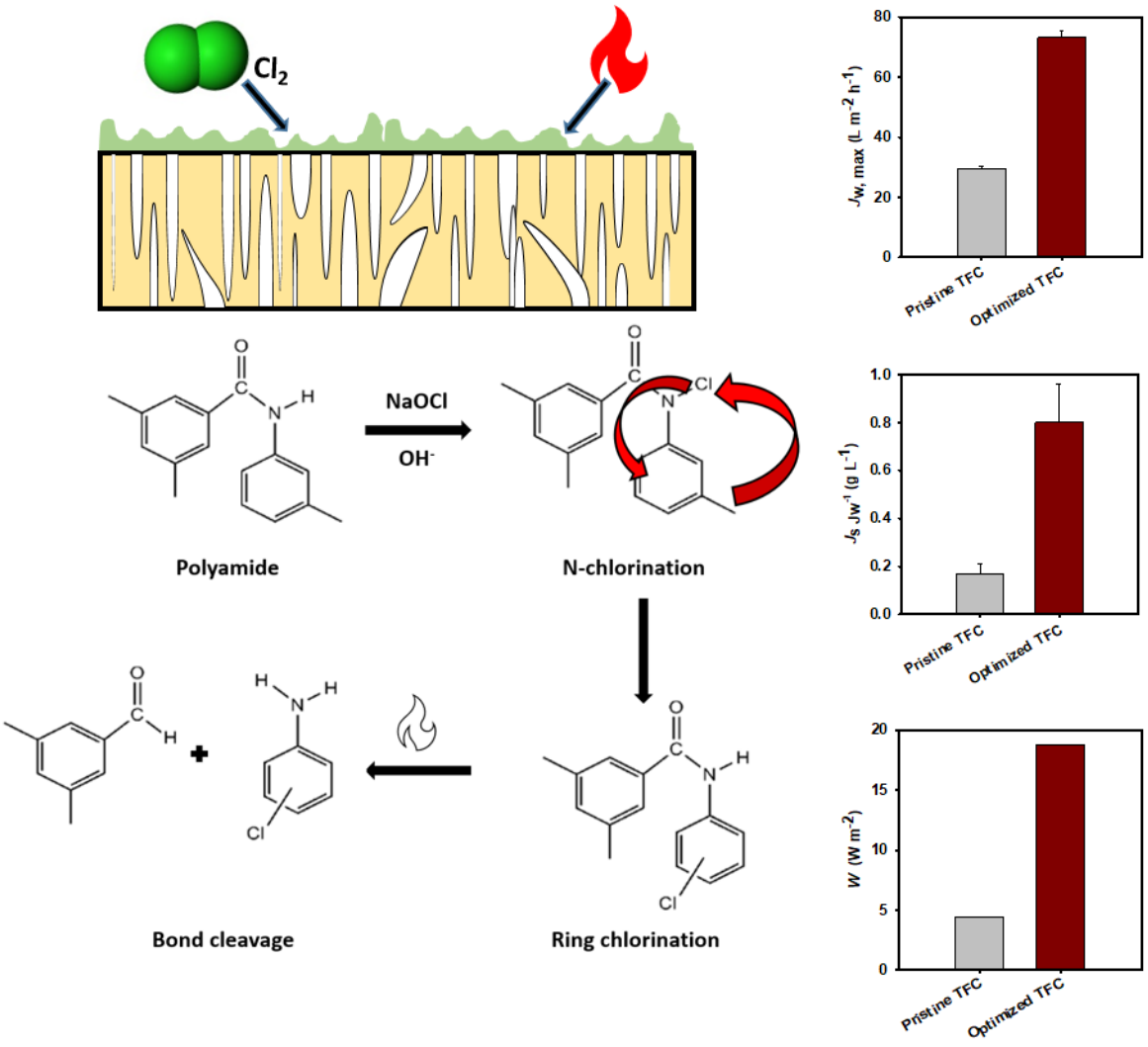

## 1. Introduction

Pressure retarded osmosis (PRO) is an osmotic-driven membrane process that has the potential to harvest renewable energy from the salinity difference between the two sides of the membrane. PRO uses the solute concentration difference between two streams of different salinities [1, 2]. The solution with low concentration of solute (feed solution, FS) passes through an asymmetric membrane towards the direction of the solution with higher solute concentration (draw solution, DS). Unlike in forward osmosis which applies little to no pressure, hydraulic pressure is applied on the DS side during PRO, against the direction of the solute concentration difference. This then impedes the flow of water from the FS toward the DS, hence naming the process pressure retarded osmosis. The mixing of the DS and FS leads to production of free energy, which can be converted into mechanical energy [3, 4].

PRO uses asymmetric semi-permeable membranes, which ideally should be highly porous and hydrophilic to maximize water permeability, highly selective against solute, and mechanically stable enough to withstand the application of hydraulic pressure during PRO operation [5]. PRO membranes are typically thin film composite (TFC) membranes, which consists of a porous support layer and a dense, selective thin film formed on the interface of the porous support [6]. Membrane properties are therefore crucial in the application of the PRO process for osmotic power generation.

Surface modification is a convenient technique to alter the properties of TFC membranes. It changes the property of the membrane without changing the membrane fabrication process.

Properties of the membrane, such as hydrophilicity, surface roughness, surface porosity, and antifouling propensity, can be altered using surface modification techniques [7]. Modification of the polyamide selective layer can be made using a number of ways, which include molecular-level design [8], incorporation of nanomaterials [9, 10], polyelectrolyte layered interfacial polymerization [11, 12], surface coating or grafting [13], and chemical modification [14]. Chemical modification usually involves exposure of the polyamide selective layer on the modifying agent and removal of the remnant agent via evaporation or drying [7]. A number of chemical modification studies also required an activation step, usually through heating [15].

The chosen modifying process in this study is chemical modification using free chlorine. Free chlorine, a term coined for an aqueous solution containing hypochlorite ($OCl^-$) and is used generally for membrane recycling, particularly for end-of-life membranes [16]. TFC membranes typically have low tolerance to chlorine, such that resistance to chlorine impact has become an important aspect to consider in manufacture of TFC membranes [17]. Chlorine exposure was found to lead to polyamide degradation, and the chlorine attack on the aromatic polyamide is known to be influenced by a number of factors, such as chlorine concentration, exposure time, pH, temperature, and pressure [18, 19]. While it had been proven that chlorine leads to deterioration of the polyamide, a controlled degree of chlorination was also found to enhance the membrane performance [20, 21]. Unlike other membrane modification techniques, chlorine modification was chosen due to its simplicity and its known effects on polyamide, which were controlled and exploited to tune the membrane transport properties.

In this study, factors influencing the heat-assisted chlorine oxidative reaction of the TFC polyamide layer, such as chlorine exposure, pH, and heating conditions. Optimization of these conditions is important to control the antagonistic effects of this modification treatment. To achieve optimization of these factors, response surface methodology (RSM), a statistical method typically used for experimental design, was employed. RSM allows to determine the interactions and the quadratic effects of various factors in an experiment. Evaluation of the significance of individual experimental factors and optimization of experimental conditions can also be performed using RSM [22]. A central composite design (CCD) contains center points and axial points, which allow estimation of the process response surface.

Several research studies have been performed to elucidate the mechanism of chlorine oxidative degradation [21, 23, 24]. Although these studies reported the mechanism of the chlorine oxidation, they did not consider the effect of other important factors, such as heat, which was explored in this work. To the best of the authors' knowledge, this is also the first study using a systemic experimental design to determine the individual and synergistic effects of the chlorine oxidation factors and how each factor could affect the polyamide integrity and TFC membrane performance. This study acknowledges that chlorine oxidation would definitely result in a decrease in selectivity, and realizing the known trade-off of permeability and selectivity, chlorine oxidative conditions were optimized to find the adequate conditions to maximize water permeability, without totally sacrificing the membrane selectivity.

Unlike variation in chlorine exposure, heat treatment of membranes exposed in free chlorine was not adequately investigated. This study, therefore, aims to investigate the effect of different factors such as pH, chlorine exposure, and heat treatment time, on chlorine oxidative modification of PRO TFC membranes. RSM was employed to systematically develop a central composite face-centered experimental design for the determination of the optimal chlorine oxidative conditions that maximize the PRO TFC membrane water permeability and osmotic energy harvesting capability, while minimizing detrimental effects on salt rejection, as well as membrane strength and stability.

## 2. Materials and Methods

### *2.1. Materials*

Chlorine oxidative degradation was conducted on pristine flat sheet PRO TFC membrane (Toray, South Korea). All chemicals used in this study were used as received and without further treatment. Sodium hypochlorite (NaOCl, 10-15% available chlorine, Sigma-Aldrich, Australia). Sodium chloride (NaCl, Chem-Supply, Pty. Ltd., Australia) was employed for the evaluation of the membrane PRO performance. Deionized (DI) water used during the experiment was produced by an ultrapure water system (Milli-Q, Merck Millipore, USA).

### *2.2. Chlorine oxidative degradation*

The TFC membranes used in this study were first cut into 5 cm x 8 cm coupons and rinsed with DI water prior to use. 4000 ppm $Cl_2$ solutions were initially prepared with different pH levels. NaOCl was diluted in 0.1 M $CH_3COO^-$ buffer, 0.1 M $HPO_4^{-2}/H_2PO_4^-$ buffer, and 0.1 M NaOH to

achieve pH levels of 5, 9, and 13, respectively. Chlorine exposure is a factor of the $Cl_2$ concentration, as well as the period of exposure, and is denoted in terms of ppm $Cl_2$·h. Using a single 4000 ppm $Cl_2$ solution, the period of membrane exposure was adjusted to vary the chlorine exposure. During the chlorine oxidation process, chlorine exposure was varied from 1000 to 4000 ppm $Cl_2$·h by exposing the polyamide selective layer of the membranes to 4000 ppm $Cl_2$ solution for 15 to 60 min. The membranes exposed to $Cl_2$ solution were afterwards heat-treated in an oven at 90 °C for up to 10 min (some membranes were not subjected to heat treatment). After oxidation and the subsequent heat treatment, the membranes were rinsed with and stored in DI water until use.

### *2.3. Optimization of chlorine oxidation using response surface methodology*

A central composite face-centered experimental design for the three factors (i.e. pH, chlorine exposure, and heat treatment period) was used in this study. The experimental design is shown in **Table 1**. A total of 15 experimental trials, consisted of eight trials for cubic points, six for axial points, and one center point, were performed in this study. The individual and synergistic effects of the oxidation and heat treatment factors were investigated. The performance of the treated membranes were compared with the pristine TFC PRO membrane (Sample 0).

The responses and the synergistic influences of the experimental factors were correlated using the following general quadratic equation (Eq. (1)) [25]:

$$\boldsymbol{Y = \beta_0 + \sum_{i=1}^{k} \beta_i X_i + \sum_{i=1}^{k} \beta_{ii} X_i^2 + \sum_{i<j} \beta_{ij} X_i X_j} \quad \textbf{(1)}$$

where $Y$ is the response, $\beta_0$ is the y-intercept, $\beta_i$ is the linear coefficient, $\beta_{ii}$ is the quadratic coefficient, and $\beta_{ij}$ is the interactive coefficient. Statistical analysis and modelling were conducted using Design-Expert software (Stat-Ease, USA). Two-dimensional contour plots showing the synergistic effects of the factors were also obtained from the software.

**Table 1.** Full factorial central composite face-centered experimental design for chlorine oxidative degradation of membranes.

| Run | Code Values | | | Real Values | | |
|---|---|---|---|---|---|---|
| | $X_1$ | $X_2$ | $X_3$ | pH | Heating Time (min) | $Cl_2$ Exposure (ppm $Cl_2$·h) |
| 0 | Pristine TFC membrane | | | | | |
| 1 | 0 | 0 | 0 | 9 | 5 | 2500 |
| 2 | -1 | -1 | -1 | 5 | 0 | 1000 |
| 3 | +1 | +1 | +1 | 13 | 10 | 4000 |
| 4 | -1 | +1 | +1 | 5 | 10 | 4000 |
| 5 | -1 | +1 | -1 | 5 | 10 | 1000 |
| 6 | +1 | -1 | -1 | 13 | 0 | 1000 |
| 7 | -1 | -1 | +1 | 5 | 0 | 4000 |
| 8 | +1 | +1 | -1 | 13 | 10 | 1000 |
| 9 | +1 | -1 | +1 | 13 | 0 | 4000 |
| 10 | +1 | 0 | 0 | 13 | 5 | 2500 |
| 11 | -1 | 0 | 0 | 5 | 5 | 2500 |
| 12 | 0 | +1 | 0 | 9 | 10 | 2500 |
| 13 | 0 | -1 | 0 | 9 | 0 | 2500 |
| 14 | 0 | 0 | +1 | 9 | 5 | 4000 |
| 15 | 0 | 0 | -1 | 9 | 5 | 1000 |

### *2.4. Membrane characterization*

The change in the membrane morphology was characterized using field emission scanning electron microscope (FESEM, JSF-7500F, JEOL, Tokyo, Japan) operated at an accelerating voltage of 5 kV. Prior to analysis, the samples were sputter-coated with osmium [26]. The membrane surface

chemistry was also characterized, using attenuated total reflectance- Fourier transform infrared spectroscopy (ATR-FTIR, IRAffinity-1, Shimadzu, Australia) and X-ray photoelectron spectroscopy (XPS; JPS-9010 MC, JEOL) with monochromated Al Kα X-rays. Contact angle measurements were obtained using an optical tensiometer (Theta Lite 100, Biolin Scientific, Republic of Korea) to estimate the membrane surface hydrophilicity. Surface mean roughness of the membranes was measured by atomic force microscope (AFM, Dimension 3100, Bruker, Germany). Membrane thickness was evaluated using a digital micrometer (MDH-25M High-Accuracy Digimatic Micrometer, Mitutoyo Corp., Japan) with an accuracy of ±0.5 μm by getting the average value of at least 5 measurements of the samples.

Using the atomic composition analysis results using XPS, the O/N ratio could be determined and used to evaluate the degree of cross-linkage of the TFC PRO membranes. The O/N ratio, which is known to be inversely related to degree of cross-linkage, was calculated using these equations [27]:

$$a + b = 1 \quad \textbf{(2)}$$

$$\frac{O}{N} = \frac{3a+4b}{2a+2b} \quad \textbf{(3)}$$

where a and b are the respective fractions of the cross-linked and linear portions of polyamide.

### *2.5. Evaluation of membrane mechanical stability and determination of membrane intrinsic transport properties*

Prior to osmotic tests, the membrane burst pressures were evaluated, following the method from our earlier study [28]. The membranes were subjected to an initial pressure of 2 bar with DI water facing the membrane active layer at a flow rate of 300 mL $min^{-1}$. After stabilization for 20 min, the pressure was increased to 5 bar. The pressure was afterwards increased by an increment of 1 bar, with 20 min stabilization in between each pressure, until membrane breakage occurred, signified by a huge increase in permeate weight. The membrane breakage pressure was defined as the membrane burst pressure.

The pure water permeability coefficient ($A$) of the membranes were also determined using Eqs. (4) and (5) at a pressure of 5 bar [28]:

$$\boldsymbol{J_w = \frac{\Delta V}{A_m \Delta t}} \quad \textbf{(4)}$$

$$\boldsymbol{A = \frac{J_w}{\Delta P}} \quad \textbf{(5)}$$

where $J_w$ is the water flux (L $m^{-2}$ $h^{-1}$), $\Delta V$ is the permeate volume (L), $A_m$ is the effective membrane area ($m^2$), $\Delta t$ is the operation time (h), and ΔP is the transmembrane pressure difference (bar).

The salt rejection ($R$, %) of the chlorine oxidized TFC membranes was also evaluated. 2000 ppm NaCl solution was used as the feed during operation at 5 bar. The $R$ value and the salt permeability coefficient ($B$) of the membranes were calculated using Eqs. (6) and (7):

$$\boldsymbol{R = \left(1 - \frac{C_p}{C_f}\right) x\ 100\ \%} \quad \textbf{(6)}$$

$$\boldsymbol{B = \left(\frac{1-R}{R}\right)(\Delta P - \Delta \pi) A} \quad \textbf{(7)}$$

where $C_p$ is the solute concentration of the permeate, $C_f$ is the solute concentration of the feed, and $\Delta\pi$ is the osmotic pressure difference across the membrane.

The membrane structure parameter ($S$, μm) of the TFC membranes was calculated by Eq. (8):

$$J_w = \frac{D}{S} \ln \frac{A \times \pi_D + B}{A \times \pi_F + J_w + B} \quad \textbf{(8)}$$

where $D$ is the solute diffusion coefficient, and $\pi_D$ and $\pi_F$ represent the respective osmotic pressures of the draw and feed solutions [3, 9].

### *2.6. Membrane osmotic performance testing*

Osmotic performance was used to evaluate the effect of chlorine oxidation on the membranes properties. The PRO performance of the membranes was tested using a bench-scale PRO system (Cheon Ha Heavy Industries Co. Ltd., Republic of Korea). 0.6 M NaCl was chosen as the DS, and DI water was used as FS. The membrane orientation was consistently AL-DS (active layer facing the DS stream) all throughout the study. The flow rate was set at 300 mL $min^{-1}$ for both streams. The membranes were first operated for FO (no applied hydraulic pressure) and the pressure was increased in intervals and stabilized for 30 min for each pressure. The PRO water flux was calculated using Eq. (4). The maximum water flux value was obtained during the initial FO operation, during which no hydraulic pressure was applied. The reverse salt flux ($J_s$, g $m^{-2}$ $h^{-1}$) was calculated using:

$$\boldsymbol{J_s = \frac{\Delta(C_t V_t)}{A_m \Delta t}} \quad \textbf{(9)}$$

where $C_t$ is the change in salt concentration and $V_t$ is the change in feed volume at time $t$. Power density ($W$, W m$^{-2}$) was determined using:

$$\boldsymbol{W = J_w \Delta P} \quad \textbf{(10)}$$

where $\Delta P$ is the pressure difference across the membrane.

## 3. Results and Discussion

### *3.1. Mechanism of chlorine oxidation*

The mechanistic approach of chemical modification is based on the interaction forces, such as π-π interactions and hydrogen bonding, between the chemical agent and the organic membrane surface, as shown in Scheme 1. Chlorine oxidation of the polyamide aromatic ring subsequently allows the deterioration of the H-bonds. The N-H bond is broken as a chlorinated N intermediate is formed due to replacing hydrogen by chlorine prior to the rearrangement into a chlorinated ring product. At harsh chlorine oxidation conditions, it is possible that bond cleavage at the chlorinated ring would occur. Also, breaking the polyamide H-bonds will lead to increased rotational freedom of the polymer chains, which could contribute to increased water permeability [20].

Upon exposure to free chlorine, the amide nitrogen (-C(=O)-N=) is first chlorinated, then the chlorine moves towards the aromatic ring via the intramolecular Orton rearrangement mechanism [29]. Moreover, the amide group is simultaneously hydrolyzed during the process, producing carboxylate and either amine or ammonia. These groups are known to be more hydrophilic compared to polyamide, which enhances the membrane's water permeability [30].

Due to the hydrolysis of amide functional groups occurring during chlorine oxidation, the acyl groups of polyamide are dissociated into ionized species, making the polyamide layer looser and more susceptible to the passage of water molecules and hydrated ions. This is among the reasons why chlorine oxidation leads to enhancement of both water and solute permeability. This dissociation of the acyl groups can be facilitated further by heat treatment, resulting in scission and bond cleavage.

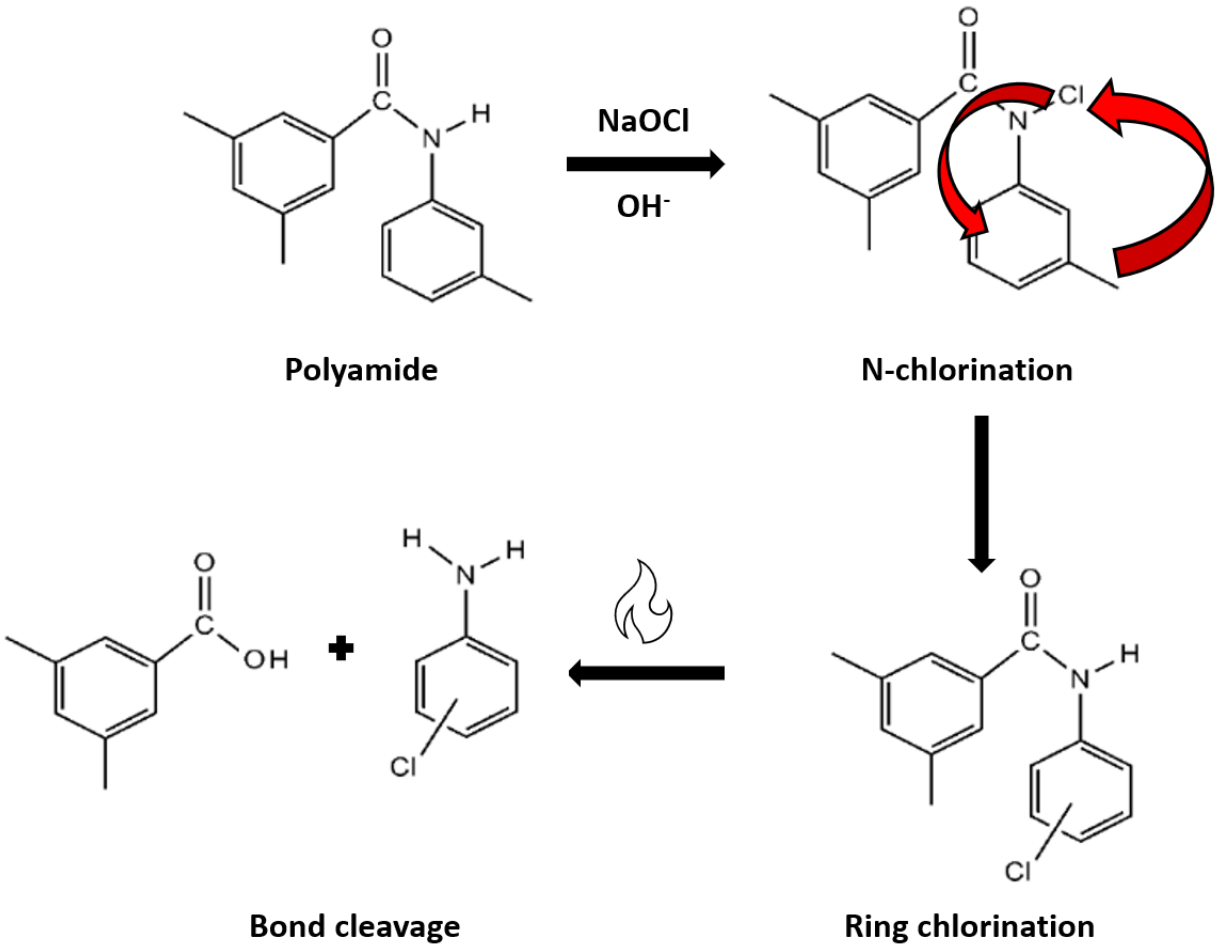

**Scheme 1.** The proposed mechanism of chlorine oxidative degradation and heat treatment on polyamide.

### *3.2. Membrane characterization and intrinsic transport properties*

Polyamide degradation and the membrane surface chemistry was confirmed using ATR-FTIR spectroscopy. Figure 1 shows the (a) FTIR and (b) XPS spectra of the pristine PRO TFC membrane and three chosen representative membranes: membrane 2 (all factors corresponding to -1; pH 5, 1000 ppm $Cl_2$·h, no heating), membrane 1 (all factors corresponding to 0; pH 9, 2500 ppm $Cl_2$·h, 5 min heating), and membrane 3 (all factors corresponding to +1; pH 13, 4000 ppm $Cl_2$·h, 10 min heating). Table 2 presents the surface elemental composition and the degree of cross-linkage of the pristine and representative modified PRO TFC membranes.

Figure 1a shows the difference in the surface chemistry of the membranes treated at different chlorine oxidation severity, compared with the pristine PRO TFC membrane. The following peaks were observed to decrease in intensity as severity increases: 1645 $cm^{-1}$ corresponding to the C=O stretching of amide, 1590 $cm^{-1}$ corresponding to the C=C stretching vibrations from aromatic polyamide, and 1541 $cm^{-1}$ corresponding to the amide N—H bond. The strength decrease at these peaks indicates that the H-bonds of the amide groups are broken due to the chlorination of N [30, 31]. These changes in the FTIR spectra indicate that there are changes in the intermolecular and intramolecular interactions of the TFC membranes [32]. All samples exhibited a small peak at around 1700 cm-1, which corresponds to carboxyl C=O. The change in intensity of the amide N-

H stretching (approximately at 1540 $cm^{-1}$) for all the modified TFC membranes evidently show the occurrence of Orton rearrangement as earlier explained and shown in Scheme 1.

XPS analysis was conducted to further elucidate the effect of chlorine oxidation on the PRO TFC membrane surface chemical composition. Figure 1b shows the XPS wide-scan and narrow-scan spectra of the pristine and representative modified PRO TFC membranes. The $C_{1s}$, $O_{1s}$, and $N_{1s}$ peaks of all membranes observed from XPS analysis are attributed to the polyamide layer. The XPS spectra showed that the $N_{1s}$ peak intensity decreased for all modified membranes It can be noticed from Table 2, however, that the modified membranes exhibited higher surface oxygen content, which could be due to the deterioration of the acyl groups of polyamide during chlorine oxidation.

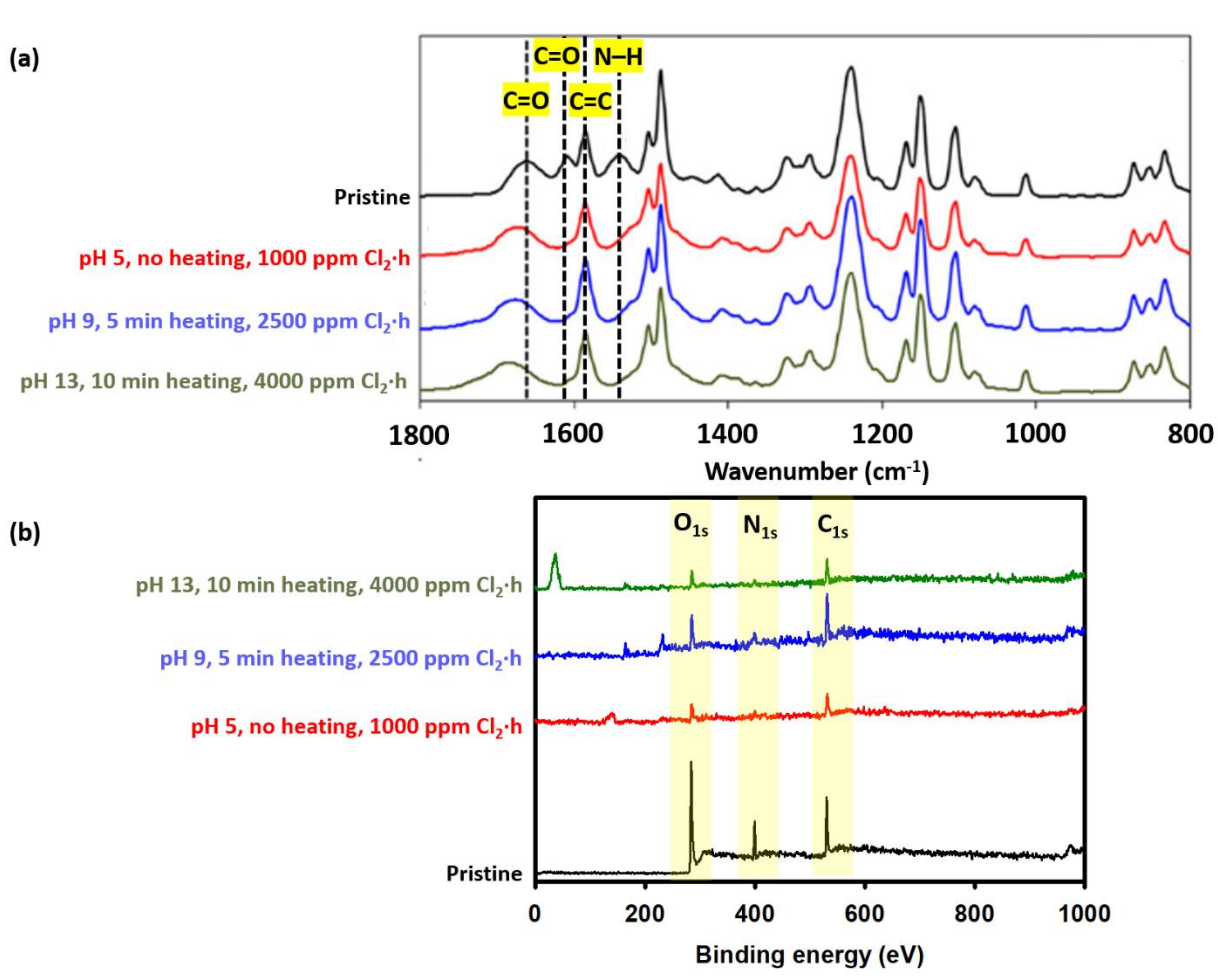


277

278 **Figure 1.** (a) FTIR and (b) XPS spectra of the pristine PRO TFC membrane and three chosen

279 representative membranes with different severity of chlorine oxidative degradation conditions.

**Table 2.** Surface elemental composition and degree of cross-linkage of pristine and modified PRO TFC membranes.

| Sample | C (%) | N (%) | O (%) | O/N | Degree of cross-linkage |
|---|---|---|---|---|---|
| 0 | 71.68 | 13.57 | 14.75 | 1.09 | 0.87 |
| 1 | 69.76 | 12.23 | 18.01 | 1.47 | 0.43 |
| 2 | 68.88 | 14.99 | 16.13 | 1.08 | 0.88 |
| 3 | 66.63 | 12.54 | 20.83 | 1.66 | 0.26 |
| 4 | 79.20 | 13.10 | 17.70 | 1.35 | 0.55 |
| 5 | 67.79 | 14.86 | 17.35 | 1.17 | 0.76 |
| 6 | 71.26 | 12.03 | 16.71 | 1.39 | 0.51 |
| 7 | 68.82 | 14.27 | 16.91 | 1.19 | 0.74 |
| 8 | 73.8 | 10.22 | 15.98 | 1.56 | 0.34 |
| 9 | 68.48 | 12.93 | 18.59 | 1.44 | 0.46 |
| 10 | 78.91 | 8.09 | 13.00 | 1.61 | 0.30 |
| 11 | 73.14 | 11.66 | 15.20 | 1.30 | 0.61 |
| 12 | 75.17 | 13.84 | 20.99 | 1.52 | 0.38 |
| 13 | 68.11 | 14.10 | 17.79 | 1.26 | 0.65 |
| 14 | 68.41 | 13.97 | 17.62 | 1.26 | 0.65 |
| 15 | 66.26 | 14.20 | 19.54 | 1.38 | 0.52 |

Hydrophilicity of the membranes were assessed through sessile drop contact angle measurements and the surface roughness of the pristine TFC membrane and three chosen representative membranes were evaluated using AFM, and the results of these characterizations are shown in Figure 2 and Table 3, respectively. Contact angle values significantly decreased after all chlorination experiments, indicating that the chlorine oxidation caused the polyamide rings to open and expose the hydrophilic functional groups on the TFC membrane surface. The increase in hydrophilicity after modification, as indicated by the decrease in water contact angle of the TFC membrane surface, show the various degrees of hydrolysis and oxidative degradation the TFC membranes have undergone due to the reaction with $Cl_2$ and the subsequent heating. The slightly hydrophobic quality of the polyamide selective layer was proven by its water contact angle of 104º. After hydrolysis and oxidative degradation, the formation of the more hydrophilic functional

groups (Scheme 1) resulted in lower contact angle measurements, despite the marked decrease in surface roughness (Table 3).

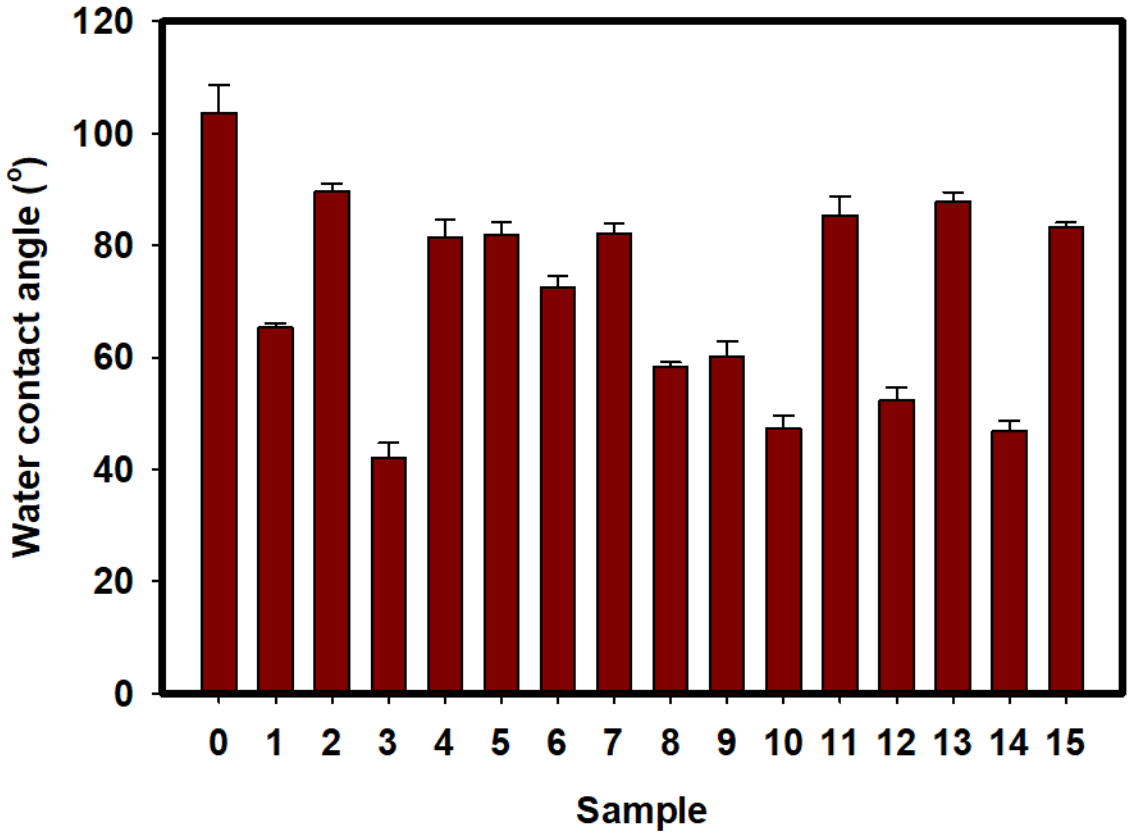


**Figure 2.** Sessile water contact angle measurements of the pristine TFC membrane and TFC membranes subjected to chlorine oxidative degradation.

**Table 3.** Surface roughness of pristine and modified PRO TFC membranes.

| Sample | $R_a$ (nm) |
|---|---|
| 0 | 10.6 ± 1.4 |
| 1 | 8.7 ± 0.3 |
| 2 | 8.4 ± 0.6 |
| 3 | 7.5 ± 0.9 |
| 4 | 9.2 ± 0.8 |
| 5 | 8.6 ± 0.7 |
| 6 | 7.8 ± 0.3 |
| 7 | 8.1 ± 1.3 |
| 8 | 9.2 ± 0.4 |
| 9 | 6.5 ± 1.7 |
| 10 | 7.7 ± 1.3 |
| 11 | 8.9 ± 1.3 |
| 12 | 8.2 ± 1.5 |
| 13 | 7.6 ± 0.7 |
| 14 | 7.8 ± 0.9 |
| 15 | 8.9 ± 0.8 |

Figure 3 shows the polyamide selective layer surface of the pristine PRO TFC membrane and three representative membranes with varying degree of severity of chlorine oxidative degradation conditions: membrane 2 (all factors corresponding to -1; pH 5, 1000 ppm $Cl_2$·h, no heating), membrane 1 (all factors corresponding to 0; pH 9, 2500 ppm $Cl_2$·h, 5 min heating), and membrane 3 (all factors corresponding to +1; pH 13, 4000 ppm $Cl_2$·h, 10 min heating). The complete FESEM images showing the surface morphology of the pristine and modified TFC membranes are shown in the Supplementary Information (Figure S1).

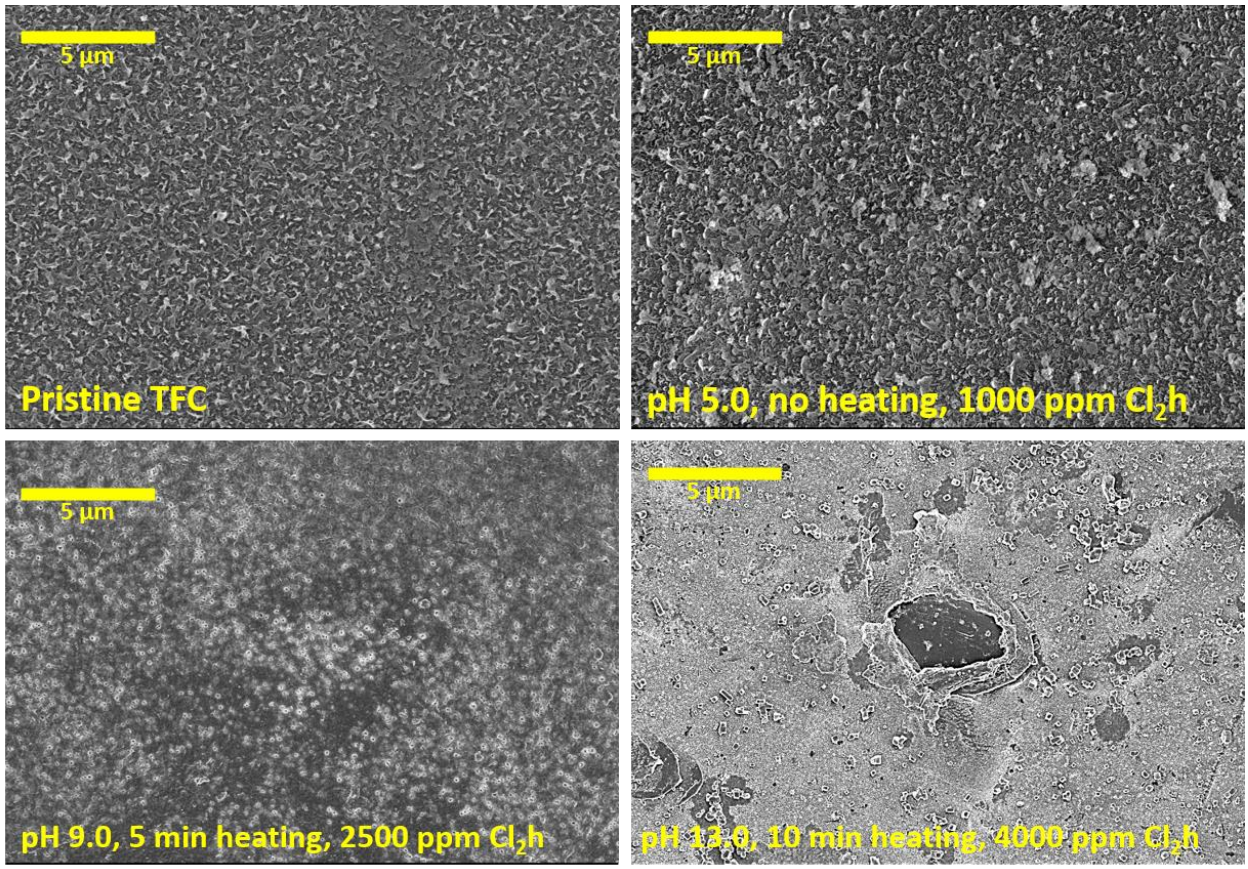


**Figure 3.** Surface morphology of the pristine PRO TFC membrane and three representative membranes with different severity of chlorine oxidative degradation conditions, as evaluated by FESEM imaging.

The surface morphologies of the PRO TFC membranes shown in Figure 3 exhibit various degrees of polyamide degradation as the condition severity increased. The polyamide layer of the pristine TFC membrane exhibited a dense, ridge-and-valley structure, typically observed with the polyamide active layer. After modification, the polyamide layers of the modified TFC membranes exhibited looser and smooth structures, depending on the oxidation severity. The PRO TFC membrane treated at acidic pH, low free chlorine exposure and no heat treatment show almost

similar ridge-and-valley structure with that of the pristine PRO TFC membrane, indicating little to no degradation of the polyamide structure. As the severity of the chlorine oxidation conditions increase, we observe the loosening of the polyamide structure, indicating the damage sustained by the polyamide due to the degradation process. The TFC membrane treated at pH 9, 2500 ppm $Cl_2$·h exposure, and 5 min heating showed smoother and melted-looking protrusions on the membrane surface. The same morphology was observed for a number of other membranes treated at intermediate chlorine oxidation severity, as shown from Figure S1. The membrane treated at the extreme chlorine oxidative degradation conditions (pH 13, 4000 ppm $Cl_2$·h exposure, and 10 min heat treatment) was observed to sustain a high degree of polyamide degradation. The looser structure of the polyamide active layer observed from the modified TFC membranes could lead to more transportation spaces and less transport resistance [15], significantly affecting membrane performance, which will be discussed in detail in the succeeding subsections.

### *3.3. Influence of chlorine oxidative degradation on TFC membrane stability*

The TFC membrane stability and mechanical properties were also evaluated. It is highly important to determine how the chemical treatment affects the stability of TFC PRO membranes and their ability to withstand the application of hydraulic pressure, especially that degradation occurs directly on the polyamide selective layer.

An important aspect of this study is the inclusion of heat in the chlorine oxidation modification process. Prior to the implementation of the experimental design and optimization of heat-assisted chlorine oxidative treatment of the TFC membranes, chlorine oxidation was first carried out using

1000 ppm $Cl_2$·h exposure at pH 9, followed by heating for 5 min at different temperatures (50, 70, and 90ºC). Both membranes treated with chlorine and heated at 50 and 70ºC exhibited marginal changes in performance during FO operation at AL-DS orientation, compared with the pristine TFC membrane, as shown in the Supplementary Information (Figure S2). Due to this set of preliminary experiments, heating temperature was set at 90ºC for all tests, varying only the length of heating.

Membrane morphology characterization via FESEM has shown that $Cl_2$ oxidation of the PRO TFC membranes have affected the integrity of the polyamide layer. To determine whether $Cl_2$ oxidation could affect the properties of TFC membrane support layer, the thickness of the pristine and modified TFC membranes were measured and presented in Figure S3. There was no significant change in the TFC membrane thickness after $Cl_2$ treatment, as shown by the results.

The burst pressure was first determined for the 15 resultant membranes obtained during the chlorine oxidative degradation process, and the burst pressures are shown in the Figure 4. As shown in the figure, the membranes resulting from the chemical oxidative degradation process exhibited burst pressures in the range of 6 to 15 bar. Chlorine oxidation definitely affects the membrane mechanical strength as a result of decreasing the polyamide active layer integrity. While the support layer stability of the TFC membranes are not affected by the chlorine oxidation, the bond breaking and scission which occurred during the modification allowed looser and less cross-linked polyamide active layers, which could not withstand the application of hydraulic pressure. These are significantly lower compared to the burst pressure of the pristine PRO TFC membrane,

364 which is 22 bar. Amongst the 20 different membrane samples tested, three membranes exhibited
365 a burst pressure of only about 6 bar: membranes 3 (pH 13, 4000 ppm $Cl_2$·h, and 10 min heating
366 time), 8 (pH 13, 1000 ppm $Cl_2$·h, and 10 min heating time), and 10 (pH 13, 2500 ppm $Cl_2$·h, and
367 5 min heating time). This agrees with the hypothesis of this study, since all these three membranes
368 were treated under an extremely alkaline pH environment. As mentioned earlier, chlorine
369 oxidation mainly occurs at alkaline conditions, and the oxidation process mainly attacks the
370 integrity of the H-bonds of the polyamide. This likely led to a much thinner and weaker polyamide
371 layer, and eventually collapsed under hydraulic pressure [18]. Following the determination of the
372 burst pressure, the membranes were all tested at a pressure lower than their individual burst
373 pressures to comparatively determine the power density of the membranes for the succeeding tests.
374 The maximum operational pressure values of each membrane are shown in Table S1. It is safe to
375 note that for membranes that can withstand higher hydraulic pressures, the power density can
376 further increase at higher hydraulic pressures applied.

377

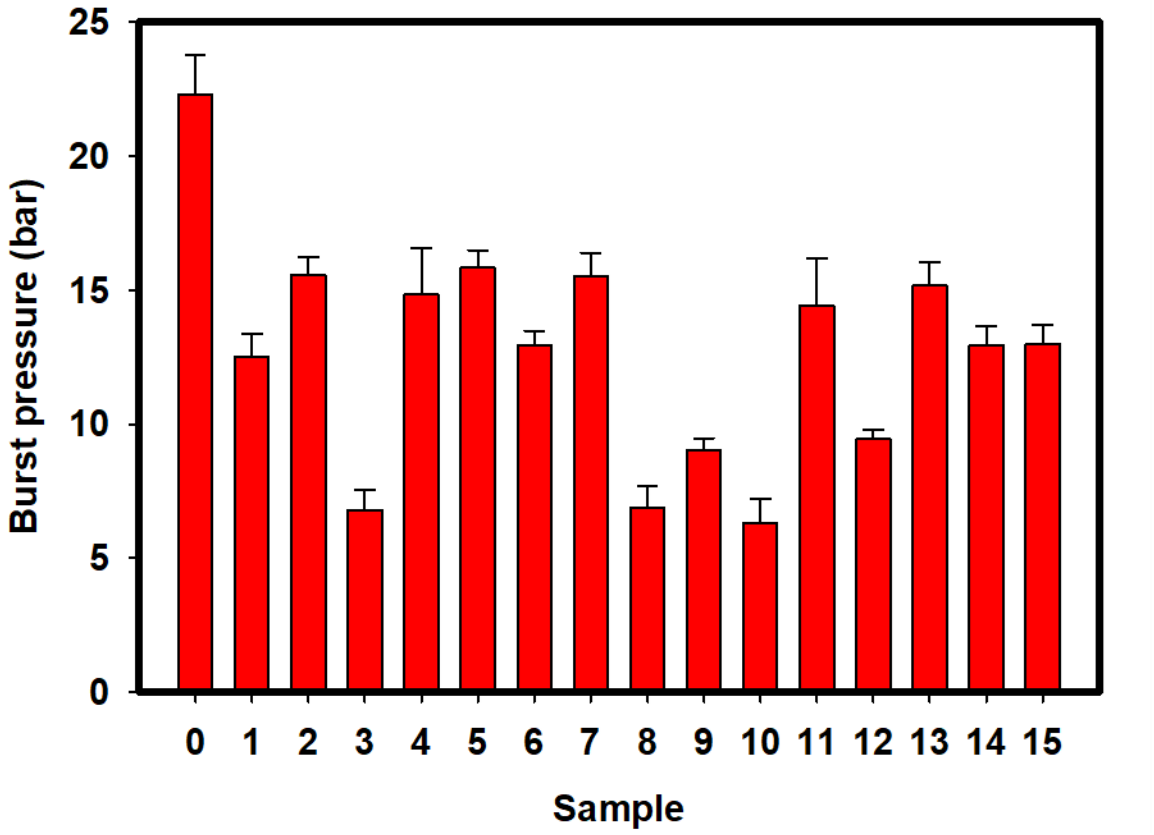


**Figure 4.** Burst pressures of the PRO TFC membranes subjected to chlorine oxidative degradation. Three membranes sustained critical damage on the polyamide layer and were observed to burst after application of hydraulic pressure of 6 bar: membranes 3 (pH 13, 4000 ppm $Cl_2$·h, and 10 min heating time), 8 (pH 13, 1000 ppm $Cl_2$·h, and 10 min heating time), and 10 (pH 13, 2500 ppm $Cl_2$·h, and 5 min heating time).

A previous study correlated the changes in mechanical properties of aromatic polyamide upon chlorine treatment [33]. Aromatic polyamide is known to be more susceptible to chlorine oxidation due to the presence of π—π interactions, resulting in increased brittleness and fragility of polyamide. Furthermore, in cases of extreme chlorine oxidation conditions, the chain breakage of

389 polysulfone is possible [34], and may lead to a significant decrease in membrane stability. This
390 was not observed in this study, due to the controlled chlorine oxidative degradation conditions
391 applied.

392

393 ***3.4. Optimization of chlorine oxidative degradation conditions***

394 In this study, the following conditions were controlled in the optimization of chlorine oxidative
395 degradation: free chlorine exposure (a factor of free chlorine dosage and exposure period), solution
396 pH, and heat treatment period. A fixed dose of 4000 ppm free chlorine was utilized for all runs,
397 and the exposure period was varied to demonstrate the effect of chlorine exposure on the TFC
398 membranes. At a fixed dosage of chlorine, a longer exposure time leads to a higher total free
399 chlorine exposure, expressed in terms of ppm $Cl_2$·h. RSM was used to find the best conditions to
400 ensure enhancement of permeability, while still having satisfactory rejection. Prior to FO operation
401 using the pristine and modified membranes, the intrinsic transport parameters (*A*, *B*, and *S* values)
402 of the membranes were first determined experimentally and presented in Table 4.

403 **Table 4.** Intrinsic transport parameters of the pristine and modified PRO TFC membranes.

| | pH | Heating Time (min) | $Cl_2$ Exposure (ppm $Cl_2$·h) | *A* (L $m^{-2}$ $h^{-1}$ $bar^{-1}$) [a] | *B* (L $m^{-2}$ $h^{-1}$) [b] | *B/A* (bar) | S (μm) |
|---|---|---|---|---|---|---|---|
| **0** | Pristine | | | 1.36 ± 0.12 | 0.44 ± 0.06 | 0.32 | 155 |
| **1** | 9 | 5 | 2500 | 2.64 ± 0.32 | 2.31 ± 0.18 | 0.88 | 101 |
| **2** | 5 | 0 | 1000 | 1.82 ± 0.15 | 1.12 ±0.09 | 0.62 | 204 |
| **3** | 13 | 10 | 4000 | 4.11 ± 0.89 | 9.87 ± 1.53 | 2.40 | 59 |
| **4** | 5 | 10 | 4000 | 2.19 ± 0.28 | 1.87 ± 0.14 | 0.85 | 140 |
| **5** | 5 | 10 | 1000 | 2.09 ± 0.09 | 1.63 ± 0.11 | 0.78 | 182 |
| **6** | 13 | 0 | 1000 | 2.46 ± 0.18 | 3.06 ± 0.29 | 1.24 | 124 |
| **7** | 5 | 0 | 4000 | 2.18 ± 0.25 | 1.42 ± 0.14 | 0.65 | 161 |
| **8** | 13 | 10 | 1000 | 3.05 ± 0.37 | 4.81 ± 0.52 | 1.58 | 95 |
| **9** | 13 | 0 | 4000 | 2.98 ± 0.17 | 3.95 ± 0.41 | 1.33 | 107 |
| **10** | 13 | 5 | 2500 | 3.91 ± 0.33 | 6.58 ± 0.79 | 1.68 | 92 |
| **11** | 5 | 5 | 2500 | 1.94 ± 0.22 | 1.50 ± 0.28 | 0.77 | 148 |
| **12** | 9 | 10 | 2500 | 3.43 ± 0.81 | 4.48 ± 0.97 | 1.31 | 103 |
| **13** | 9 | 0 | 2500 | 2.27 ± 0.40 | 1.95 ± 0.38 | 0.86 | 132 |
| **14** | 9 | 5 | 4000 | 3.86 ± 0.56 | 2.52 ± 0.67 | 0.65 | 92 |
| **15** | 9 | 5 | 1000 | 2.61 ± 0.43 | 2.11 ± 0.74 | 0.81 | 133 |

404 [a] Feed solution: DI water; applied pressure: 5 bar

405 [b] Feed solution: 2000 ppm NaCl; applied pressure: 5 bar

The pristine TFC membrane exhibited pure water permeability of 1.36 L $m^{-2}$ $h^{-1}$ $bar^{-1}$ and an intrinsic selectivity (*B/A*) of 0.32 bar. All the chlorine oxidation-modified membranes exhibited increase in pure water permeability, and similarly, the *B/A* values increased as well, indicating lower selectivity for all modified membranes. The enhancement of the pure water permeability of the membranes corresponded well with the increase in surface hydrophilicity of the membranes, as shown by the water contact angle measurements.

Each of the membranes were operated up until the burst pressure of each was reached to obtain the maximum extractable power density ($W_{max}$). The $W_{max}$ value of each membrane, which is influenced by the maximum operational pressure, was used for the modelling and process optimization. A summary of the osmotic performance of the membranes are provided in the Supplementary Information (Table S1).

### *3.4.1. Influence of pH and free chlorine exposure at constant heating time*

Since it was earlier established that chlorine oxidative degradation occurs specifically at alkaline pH, we first examine the influence of pH and free chlorine exposure on the PRO TFC membranes at a constant heating time of 5 min (middle factor in the RSM design). The influence of pH and free chlorine exposure on the osmotic performance of the membranes are shown in Figure 5.

Previous studies of Donose et al. [18] and Kang et al. [35] had shown the effect of pH on RO membrane ageing after exposure to hypochlorite. In their study, it was found that the effect of

hypochlorite ($OCl^-$) treatment on polyamide is preferred in alkaline environment, just as most oxidation reactions occur preferably at a specific pH. At pH levels over 8, the researchers found that the $OCl^-$ allows the swelling in the polyamide structure.

It is clearly seen from Figure 5 that at acidic pH (pH 5), the membranes showed particularly lower water flux and maximum power density, similar to that of the pristine TFC membrane, regardless of free chlorine exposure. This indicates the possibility that chlorine oxidation did not proceed due to the acidic nature of the solution. However, at higher pH, it can be seen that the water flux and power density values dramatically increased until pH 13, with highest water flux and power density values when the membrane was also exposed at 4000 ppm $Cl_2 \cdot h$. The specific reverse salt flux, on the other hand, is found to be moderately affected by both pH and free chlorine exposure. Albeit typically high $J_s J_w^{-1}$ values were observed at higher pH and free chlorine exposure (0.75 to 2.57 g $L^{-1}$), these were not the highest $J_s J_w^{-1}$ values in this study, indicating that the decrease in selectivity of the membranes are mainly due to the occurrence of oxidation reaction.

As shown from Figure 5, there was a drop in the membrane selectivity (marked by increase in $J_s$ $J_w^{-1}$ value) for the membrane particularly treated at high chlorine exposure and pH. The rejection of the chlorine oxidized membranes is like that of nanofiltration (NF) membranes whose polyamide selective layer are looser than those of FO and RO. This sharp drop in solute rejection is a clear sign that the polyamide layer has sustained damage not only from chlorine oxidation, but also due to the bond breaking during heat treatment. As shown from the FESEM images (Figure 3), the various conditions of chlorine oxidation treatment resulted in changes in the TFC membrane

surface morphology, indicating the change in the integrity of the polyamide selective layer. Elemental composition analysis results obtained from XPS (Table 2) also indicate the decrease in polyamide cross-linkage of the TFC membranes, which could inevitably cause the drop in rejection of the chlorine-treated membranes [27].

### *3.4.2. Influence of pH and heating time at constant free chlorine exposure*

The influence of pH and heating time on the osmotic performance of the PRO TFC membranes at constant free chlorine exposure of 2500 ppm $Cl_2$·h (middle factor in RSM design) is shown in Figure 6.

Figure 6 shows that both pH and heating time have moderate influence on the osmotic performance of the membranes exposed to free chlorine at 2500 ppm $Cl_2$·h. Moderate increase (indicated by blue- and green-colored regions in the contour plots ) indicate a lower degree of polyamide degradation. For membranes exposed to high concentration of free chlorine and shorter exposure times, the polyamide is not fully degraded. Consistently with pH being an important parameter in oxidative reactions, it can also be seen from these results that at acidic pH, low water flux and maximum power density values were observed.

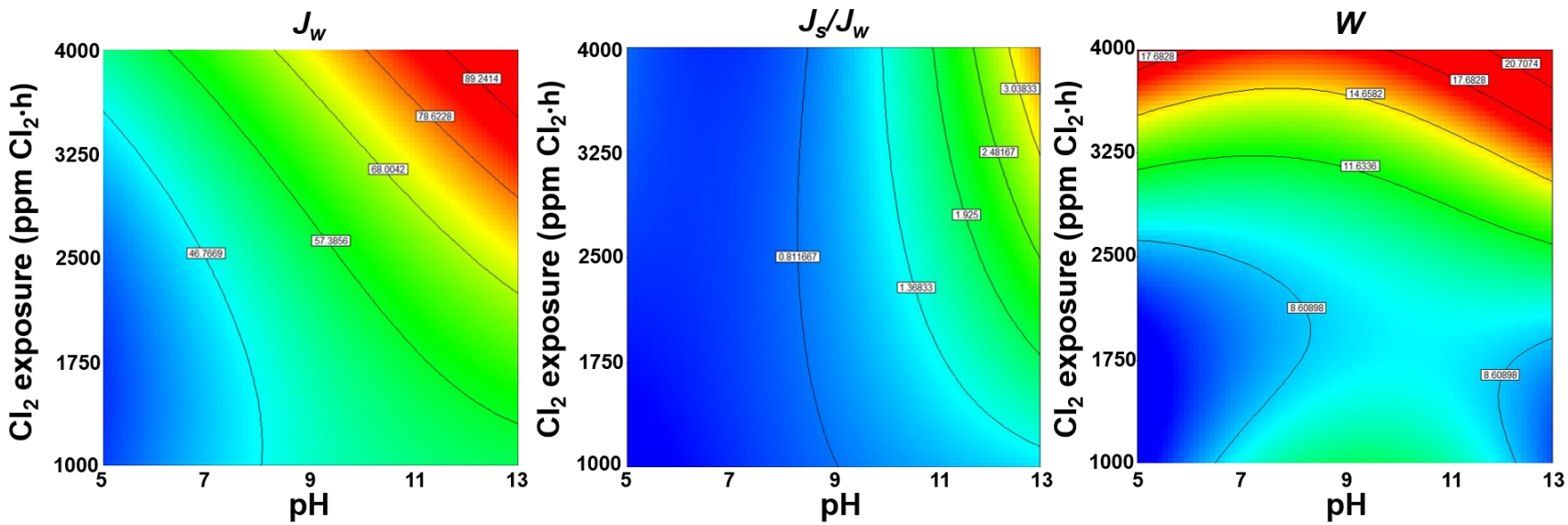


466

467 **Figure 5**. Contour plots (generated using Design-Expert 7.0.0) showing the influence of pH and free chlorine exposure on the water
468 flux, specific reverse salt flux, and power density, at constant heating time of 5 min.

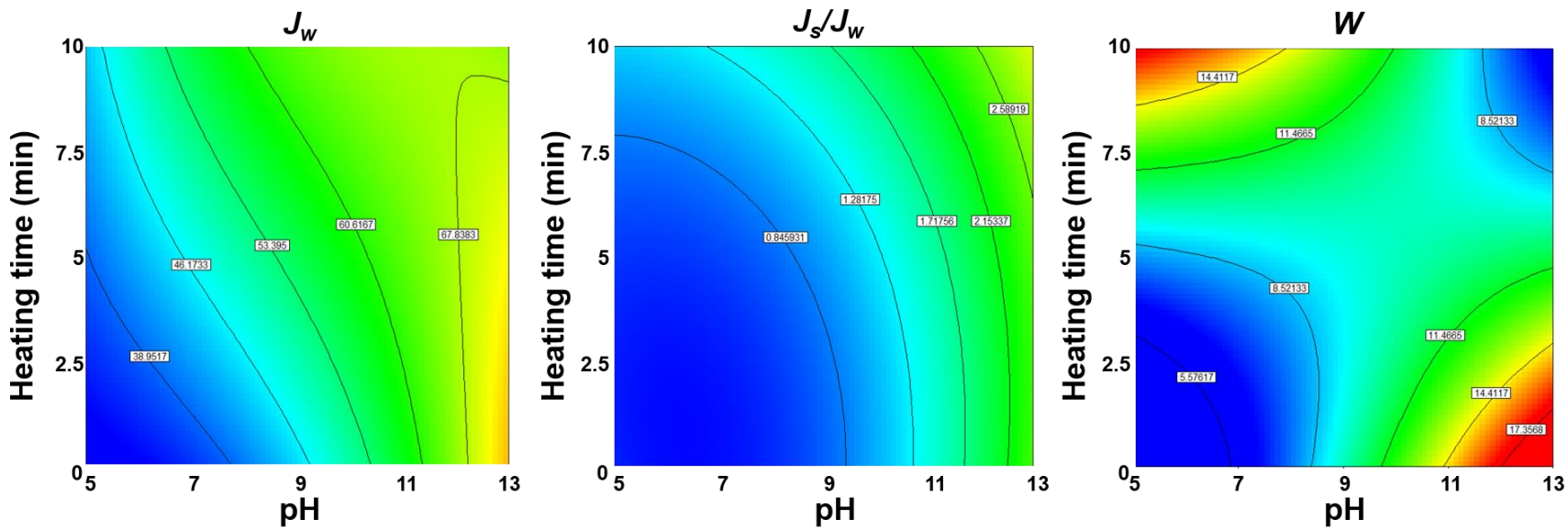


**Figure 6.** The contour plots (generated using Design-Expert 7.0.0) showing the influence of pH and heating time on the water flux, specific reverse salt flux, and power density, at constant free chlorine exposure of 2500 ppm.

### *3.4.3. Influence of free chlorine exposure and heating time at constant pH*

Lastly, the influence of free chlorine exposure and heating time on the osmotic performance of the PRO TFC membranes at constant pH of 9 (middle factor in RSM design) is shown in Figure 7.

At a constant alkaline pH of 9, we can now see how free chlorine exposure and the downstream heat treatment affect the membranes' osmotic performance. It is interesting to note that at lower free chlorine exposure and short to no heat treatment, chlorine oxidation did not necessarily affect the membrane permeability and selectivity. Garcia-Pacheco et al [16] earlier reported that low chlorine exposure levels (around 50 – 1000 ppm $Cl_2 \cdot h$) would lead to an increase in the water permeability of the membrane without affecting the solute rejection significantly. At high free chlorine exposure and long heating period, there was definitely a marked increase in both water flux and maximum power density, while keeping solute rejection moderately affected. In the case of power density, the highest power density values were marked at high chlorine exposure, regardless of heating time.

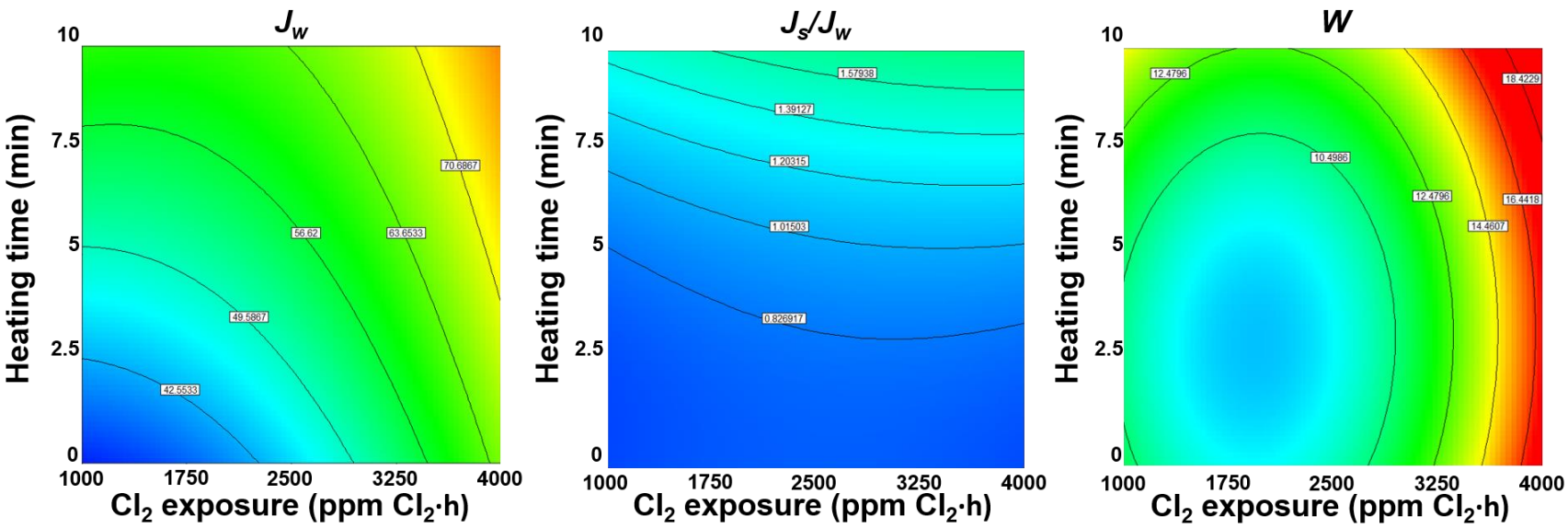


**Figure 7.** The contour plots (generated using Design-Expert 7.0.0) showing the influence of free chlorine exposure and heating time on the water flux, specific reverse salt flux, and power density, at constant pH of 9.

### *3.4.4. Synergistic effect of the chlorine oxidation factors and optimization of chlorine oxidation*

The membrane performance is presented in two-dimensional contour plots (**Figures 5** to **7**) which model the synergistic effects of two experimental factors when a third factor is held constant. The contour plots show that all three factors — free chlorine exposure, pH, and heat treatment time — have significant individual impacts on the PRO TFC membrane performance. These results indicate that tuning the structure of the polyamide selective via chemical modification can significantly affect membrane performance.

RSM was used to optimize the chlorine oxidative degradation conditions and model their synergistic effect on the following osmotic performance parameters: water flux, specific reverse salt flux, and power density. The following are the regression equations of water flux ($J_w$), reverse salt flux ($J_s\ J_w^{-1}$), and power density ($W$) obtained during RSM optimization (Regression coefficient values are also indicated):

$$J_w = 16.20 + 4.07\,x - 6.55\text{x}10^{-3}\,y + 1.64\,z + 5.35\text{x}10^{-4}\,xy - 0.05\,xz + 1.42\text{x}10^{-4}\,yz - 0.13\,x^2 + 1.46\text{x}10^{-6}\,y^2 - 0.12\,z^2 \qquad \mathbf{R^2 = 0.9971} \qquad \mathbf{9}$$

$$J_s/J_w = 2.29 - 0.55\,x - 5.89\text{x}10^{-5}\,y - 0.13\,z + 6.31\text{x}10^{-5}\,xy + 9.5\text{x}10^{-3}\,xz + 2.18\text{x}10^{-5}\,yz - 0.03\,x^2 - 6.67\text{x}10^{-8}\,y^2 + 6.79\text{x}10^{-3}\,z^2 \qquad \mathbf{R^2 = 0.9752} \qquad \mathbf{10}$$

$$W = -2.24 + 2.83\,x - 4.30\text{x}10^{-4}\,y + 0.81\,z + 1.46\text{x}10^{-6}\,xy - 0.08\,xz + 7.18x10^{-5}\,yz - 0.12\,x^2 + 1.06x10^{-6}\,y^2 - 5.77\text{x}10^{-3}\,z^2 \qquad \mathbf{R^2 = 0.9484} \qquad \mathbf{11}$$

All modelled regression equations have regression coefficient values ($R^2$) values over 0.94, indicating that the regression models accurately predict the experimental data. ANOVA results showed that the computed F-values (114.11, 13.11, and 6.13 for $J_w$, $J_s\ J_w^{-1}$, and $W$, respectively) are all greater than the tabular F-value of 2.76 at the 5% confidence interval. Moreover, the low p-

values (0.0002, 0.0119, and 0.047 for $J_w$, $J_s J_w^{-1}$, and $W$, respectively) indicate that the regression was statistically significant.

According to the optimized regression models, the membrane should be treated at the following conditions: pH 10.72, 3025 ppm $Cl_2$·h exposure, and 3 min heat treatment, to maximize $J_w$ to 78.4 L $m^{-2}$ $h^{-1}$ and power density to 20.93 W $m^{-2}$, while keeping the specific reverse salt flux ($J_s J_w^{-1}$) to 1.30 g $L^{-1}$. The optimized chlorine oxidative conditions provided by the model were applied on a pristine TFC membrane to check the validity of the optimization.

The morphology and the PRO performance of the TFC PRO membrane treated at the optimal chlorine oxidation treatment conditions are shown in Figure 8. Prior to the osmotic testing, the burst pressure was initially evaluated and found to burst at 13 bar, thus PRO testing was performed until the application of hydraulic pressure of 12 bar. The intrinsic transport parameters of the optimized modified membrane were evaluated and its pure water and solute permeability coefficients are 3.79 ± 0.83 L $m^{-2}$ $h^{-1}$ $bar^{-1}$ and 2.18 ± 0.44 L $m^{-2}$ $h^{-1}$, respectively.Operation using FO (no applied hydraulic pressure) provided the maximum non-pressure-retarded water flux of 73.2 L $m^{-2}$ $h^{-1}$ and a specific reverse salt flux of 1.17 g $L^{-1}$, which are both 93.4 and 90.1% of the values obtained from the optimization model. The maximum extractable power density was found to be 18.71 W $m^{-2}$, which is 89.4% lower than the modelled value. In terms of performance change relative to the pristine membrane, the optimized chlorine oxidation-modified TFC membrane improved the maximum non-pressure-retarded water flux by 247% and the maximum extractable power density by 420%, despite operating the modified membrane at a lower applied pressure.

535 Selectivity suffered as well with a 400% increase from that of the pristine membrane, but remains
536 satisfactory, below 1 g $L^{-1}$.

537

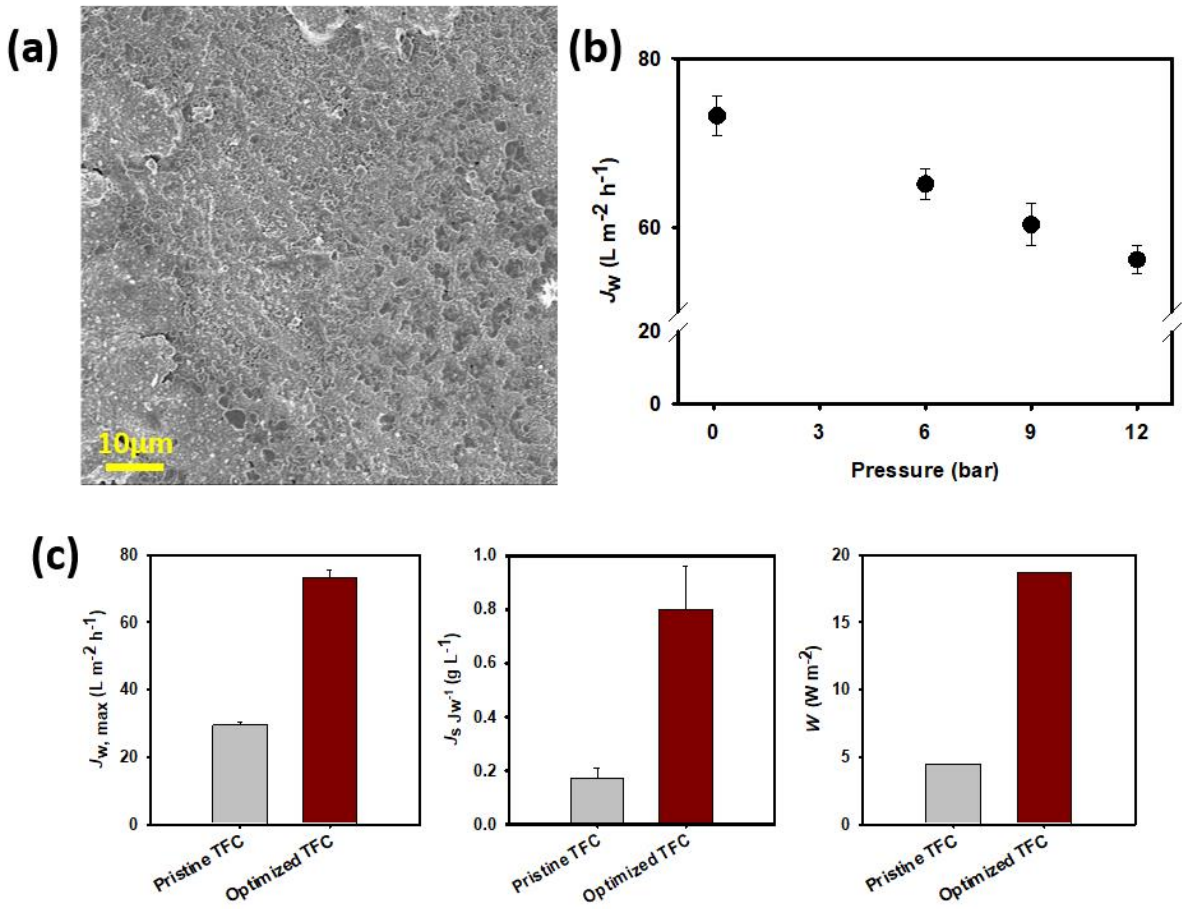


538

539 **Figure 8.** (a) Morphology and (b) PRO water flux at different applied hydraulic pressures of the
540 PRO TFC treated at optimal chlorine oxidation treatment conditions, and (c) comparison of the
541 PRO performance of the pristine TFC and the optimized chlorine oxidized TFC membranes.

542

543 **4. Conclusion**

Chlorine oxidation of the TFC membrane surface can lead to degradation of the polyamide selective layer. However, the antagonistic effects of chlorine oxidative degradation can be controlled when performed under optimal conditions to exhibit enhanced water permeability without significantly affecting solute rejection and without sacrificing its mechanical strength, to obtain a higher extractable osmotic energy from PRO membranes. The main findings from this study are:

- Significant increase in water flux and power density values were observed for membranes subjected to chlorine oxidation, but only under alkaline conditions;
- Mechanical defects and polyamide degradation caused enhanced water and solute permeability of the membranes;
- Chlorine oxidation degrades the polyamide through a chlorination on the aromatic group of the polyamide, leading to dissociation and scission; and
- Downstream heat treatment of the membranes can further cause bond cleavage on the polyamide structure.

**ACKNOWLEDGEMENT**

This research was supported by a grant from the Qatar National Research Fund under its National Priorities Research Program award number NPRP 10-1231-160069 and the Australian Research Council (ARC) Industrial Transformation Research Hub (IH170100009).

## References


[1] Q. She, X. Jin, C.Y. Tang, Osmotic power production from salinity gradient resource by pressure retarded osmosis: Effects of operating conditions and reverse solute diffusion, Journal of Membrane Science, 401 (2012) 262-273.

[2] R.R. Gonzales, A. Abdel-Wahab, S. Adham, D.S. Han, S. Phuntsho, W. Suwaileh, N. Hilal, H.K. Shon, Salinity gradient energy generation by pressure retarded osmosis: A review, Desalination, 500 (2021) 114841.

[3] F. Volpin, R.R. Gonzales, S. Lim, N. Pathak, S. Phuntsho, H.K. Shon, GreenPRO: A novel fertiliser-driven osmotic power generation process for fertigation, Desalination, 447 (2018) 158-166.

[4] H.W. Chung, L.D. Banchik, J. Swaminathan, J.H. Lienhard V, On the present and future economic viability of stand-alone pressure-retarded osmosis, Desalination, 408 (2017) 133-144.

[5] S. Zhang, P. Sukitpaneenit, T.-S. Chung, Design of robust hollow fiber membranes with high power density for osmotic energy production, Chemical Engineering Journal, 241 (2014) 457-465.

[6] N.Y. Yip, A. Tiraferri, W.A. Phillip, J.D. Schiffman, L.A. Hoover, Y.C. Kim, M. Elimelech, Thin-film composite pressure retarded osmosis membranes for sustainable power generation from salinity gradients, Environmental Science & Technology, 45 (2011) 4360-4369.

[7] D. Ankoliya, B. Mehta, H. Raval, Advances in surface modification techniques of reverse osmosis membrane over the years, Separation Science and Technology, 54 (2019) 293-310.

[8] J.L. Li, Y. Zhang, S. Zhang, M. Liu, X. Li, T. Cai, Hyperbranched poly(ionic liquid) functionalized poly(ether sulfone) membranes as healable antifouling coatings for osmotic power generation, Journal of Materials Chemistry A, 7 (2019) 8167-8176.

[9] R.R. Gonzales, M.J. Park, T.-H. Bae, Y. Yang, A. Abdel-Wahab, S. Phuntsho, H.K. Shon, Melamine-based covalent organic framework-incorporated thin film nanocomposite membrane for enhanced osmotic power generation, Desalination, 459 (2019) 10-19.

[10] R.R. Gonzales, Y. Yang, M.J. Park, T.-H. Bae, A. Abdel-Wahab, S. Phuntsho, H.K. Shon, Enhanced water permeability and osmotic power generation with sulfonate-functionalised porous polymer-incorporated thin film nanocomposite membranes, Desalination, (2020).

[11] W. Choi, S. Jeon, S.J. Kwon, H. Park, Y.-I. Park, S.-E. Nam, P.S. Lee, J.S. Lee, J. Choi, S. Hong, E.P. Chan, J.-H. Lee, Thin film composite reverse osmosis membranes prepared via layered interfacial polymerization, Journal of Membrane Science, 527 (2017) 121-128.

[12] R.R. Gonzales, M.J. Park, L. Tijing, D.S. Han, S. Phuntsho, H.K. Shon, Modification of nanofiber support layer for thin film composite forward osmosis membranes via layer-by-layer polyelectrolyte deposition, Membranes, 8 (2018) 70-84.

[13] S. Saki, N. Uzal, Surface coating of polyamide reverse osmosis membranes with zwitterionic 3-(3,4-dihydroxyphenyl)-l-alanine (l-DOPA) for forward osmosis, Water and Environment Journal, 0 (2019).

[14] S. Xiong, S. Xu, A. Phommachanh, M. Yi, Y. Wang, Versatile surface modification of TFC membrane by layer-by-layer assembly of phytic acid-metal complexes for comprehensively enhanced FO performance, Environmental Science & Technology, 53 (2019) 3331-3341.

[15] J. Zhang, Z. Qin, L. Yang, H. Guo, S. Han, Activation promoted ionic liquid modification of reverse osmosis membrane towards enhanced permeability for desalination, Journal of the Taiwan Institute of Chemical Engineers, 80 (2017) 25-33.

[16] R. García-Pacheco, J. Landaburu-Aguirre, A. Lejarazu-Larrañaga, L. Rodríguez-Sáez, S. Molina, T. Ransome, E. García-Calvo, Free chlorine exposure dose (ppm·h) and its impact on RO membranes ageing and recycling potential, Desalination, 457 (2019) 133-143.

[17] Q. Chen, F. Sun, J. Zhou, Y. Lu, Y.-Y. Li, H.-Y. Yu, J.-S. Gu, Chlorine-resistant and internal-concentration-polarization-mitigated polyamide membrane via tethering poly(ethylene glycol) methacrylate, Journal of Applied Polymer Science, 136 (2019) 47406.
[18] B.C. Donose, S. Sukumar, M. Pidou, Y. Poussade, J. Keller, W. Gernjak, Effect of pH on the ageing of reverse osmosis membranes upon exposure to hypochlorite, Desalination, 309 (2013) 97-105.
[19] J. Xu, Z. Wang, X. Wei, S. Yang, J. Wang, S. Wang, The chlorination process of crosslinked aromatic polyamide reverse osmosis membrane: New insights from the study of self-made membrane, Desalination, 313 (2013) 145-155.
[20] X. Zhai, J. Meng, R. Li, L. Ni, Y. Zhang, Hypochlorite treatment on thin film composite RO membrane to improve boron removal performance, Desalination, 274 (2011) 136-143.
[21] H.D. Raval, J.J. Trivedi, S.V. Joshi, C.V. Devmurari, Flux enhancement of thin film composite RO membrane by controlled chlorine treatment, Desalination, 250 (2010) 945-949.
[22] G. Chi, S. Hu, Y. Yang, T. Chen, Response surface methodology with prediction uncertainty: A multi-objective optimisation approach, Chemical Engineering Research and Design, 90 (2012) 1235-1244.
[23] A. Antony, R. Fudianto, S. Cox, G. Leslie, Assessing the oxidative degradation of polyamide reverse osmosis membrane—Accelerated ageing with hypochlorite exposure, Journal of Membrane Science, 347 (2010) 159-164.
[24] J.M. Gohil, A.K. Suresh, Chlorine attack on reverse osmosis membranes: Mechanisms and mitigation strategies, Journal of Membrane Science, 541 (2017) 108-126.
[25] R.R. Gonzales, J.S. Kim, S.-H. Kim, Optimization of dilute acid and enzymatic hydrolysis for dark fermentative hydrogen production from the empty fruit bunch of oil palm, International Journal of Hydrogen Energy, 44 (2019) 2191-2202.
[26] R.R. Gonzales, L. Zhang, Y. Sasaki, W. Kushida, H. Matsuyama, H.K. Shon, Facile development of comprehensively fouling-resistant reduced polyketone-based thin film composite forward osmosis membrane for treatment of oily wastewater, Journal of Membrane Science, 626 (2021) 119185.
[27] M.J. Park, C. Wang, D.H. Seo, R.R. Gonzales, H. Matsuyama, H.K. Shon, Inkjet printed single walled carbon nanotube as an interlayer for high performance thin film composite nanofiltration membrane, Journal of Membrane Science, 620 (2021) 118901.
[28] M.J. Park, S. Lim, R.R. Gonzales, S. Phuntsho, D.S. Han, A. Abdel-Wahab, S. Adham, H.K. Shon, Thin-film composite hollow fiber membranes incorporated with graphene oxide in polyethersulfone support layers for enhanced osmotic power density, Desalination, 464 (2019) 63-75.
[29] P.R. Buch, D. Jagan Mohan, A.V.R. Reddy, Preparation, characterization and chlorine stability of aromatic–cycloaliphatic polyamide thin film composite membranes, Journal of Membrane Science, 309 (2008) 36-44.
[30] V.T. Do, C.Y. Tang, M. Reinhard, J.O. Leckie, Degradation of polyamide nanofiltration and reverse osmosis membranes by hypochlorite, Environmental Science & Technology, 46 (2012) 852-859.
[31] A. Ettori, E. Gaudichet-Maurin, J.-C. Schrotter, P. Aimar, C. Causserand, Permeability and chemical analysis of aromatic polyamide based membranes exposed to sodium hypochlorite, Journal of Membrane Science, 375 (2011) 220-230.

[32] K. Hashiba, S. Nakai, M. Ohno, W. Nishijima, T. Gotoh, T. Iizawa, Deterioration mechanism of a tertiary polyamide reverse osmosis membrane by hypochlorite, Environmental Science & Technology, 53 (2019) 9109-9117.
[33] J.-H. Lee, J.Y. Chung, E.P. Chan, C.M. Stafford, Correlating chlorine-induced changes in mechanical properties to performance in polyamide-based thin film composite membranes, Journal of Membrane Science, 433 (2013) 72-79.
[34] C. Regula, E. Carretier, Y. Wyart, M. Sergent, G. Gésan-Guiziou, D. Ferry, A. Vincent, D. Boudot, P. Moulin, Ageing of ultrafiltration membranes in contact with sodium hypochlorite and commercial oxidant: Experimental designs as a new ageing protocol, Separation and Purification Technology, 103 (2013) 119-138.
[35] G.-D. Kang, C.-J. Gao, W.-D. Chen, X.-M. Jie, Y.-M. Cao, Q. Yuan, Study on hypochlorite degradation of aromatic polyamide reverse osmosis membrane, Journal of Membrane Science, 300 (2007) 165-171.